Detection and Classification of Local Ca^{2+} Release Events in Cardiomyocytes Using 3D-UNet Neural Network

Prisca Dotti[1,2], Pablo Márquez Neila[1], Miguel Fernandez-Tenorio[2], Radoslav Janicek[2], Marcel Wullschleger[2], Till Meyer zu Westram[1], Raphael Sznitman[1], Marcel Egger[2]

Affiliations:

[1]AIMI, ARTORG Center, University of Bern, Bern, Switzerland

[2]Department of Physiology, University of Bern, Bern, Switzerland

Correspondence to *prisca.dotti@unibe.ch*

UNIVERSITÄT BERN

Introduction

Global Ca^{2+} increase in the cytosol of cardiomyocytes is crucial for the contraction of the heart. Malfunctioning of proteins involved in this process can trigger local events (e.g., sparks and puffs) and global events (e.g., waves). These are thought to be involved in the development of arrhythmia. Therefore, it is important to detect and classify local Ca^{2+} release events. We present a novel approach, based on a 3D U-Net architecture, to perform these tasks in a fully automated fashion. We employed data obtained with fast xyt confocal imaging of cardiomyocytes where such subcellular Ca^{2+} events are manually annotated and trained the neural network to infer comparable segmentation as output. Despite the relatively small amount of available data and the challenges that it exhibits, we obtained qualitatively promising results.

Challenging Ca^{2+} imaging data

The main task is the detection of three types of SR-Ca^{2+} release events in atrial cardiomyocytes:

- **Ca^{2+} sparks:** coordinated opening of cluster of 6 to 20 ryanodine receptors (RyRs) triggered by calcium ions [2].

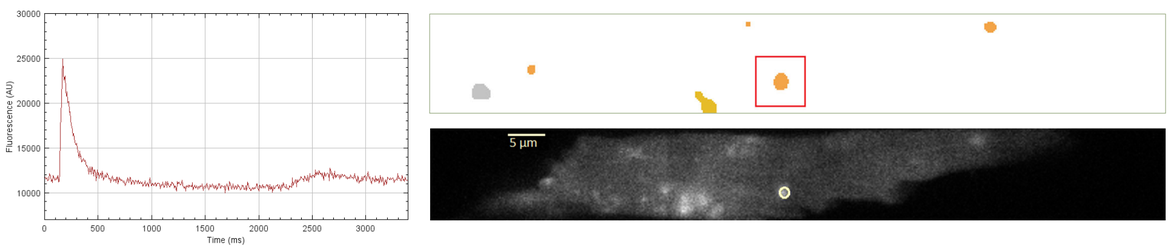

Figure 1: Signal over time of a sample Ca^{2+} spark (left). Annotation mask used for training , plotted Ca^{2+} spark is in the red box (top right). Slice of sample movie, the yellow circle denotes the region over which temporal data is averaged (bottom right).

- **Ca^{2+} puffs:** opening of 20 to 35 coordinated inositol trisphosphate receptors (InsP3Rs) [3].

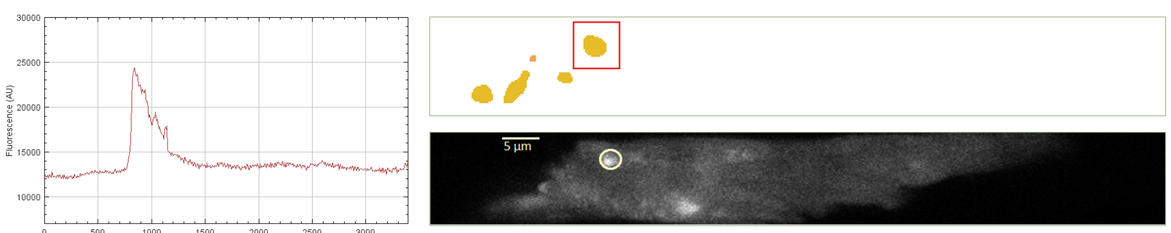

Figure 2: Signal over time of a sample Ca^{2+} puff (left). Annotation mask used for training, plotted Ca^{2+} puff is in the red box (top right). Slice of sample movie, the yellow circle denotes the region over which temporal data is averaged (bottom right).

- **Ca^{2+} waves:** propagation of Ca^{2+} sparks along the length of the cell [2].

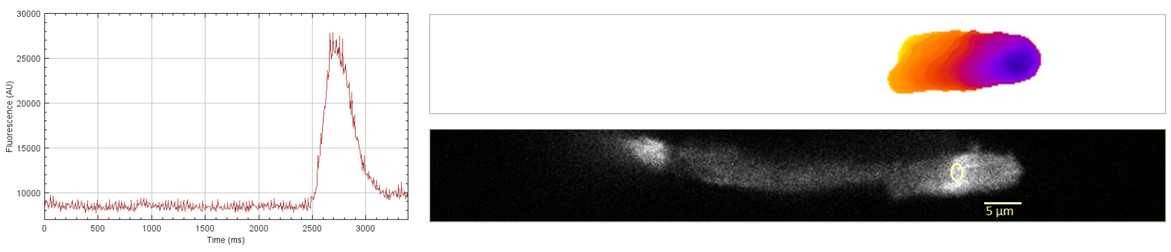

Figure 3: Signal over time of a sample Ca^{2+} wave (left). Propagation of Ca^{2+} wave in time, different colors indicate time from the start of the event. Dark purple represents the origin of the event and yellow its end (top right). Slice of sample movie, the yellow circle denotes region over which temporal data is averaged (bottom right).

- Simple thresholds on measures such as amplitude, rise and decay times, etc., are not sufficient to separate the three classes of events.
- **Crosstalks are possible between Ca^{2+} sparks and Ca^{2+} puffs** [1], making the classification task even more challenging.

The dataset consists of 43 xyt image series. Each sample contains from 500 to 1900 frames (512x64 pixels), recorded with a frequency of images between 137.5 Hz and 169.5 Hz. Pharmacology has been utilized to stimulate InsP3Rs activity in a subset of the samples, for this reason, data present different types of noise.

Method

Data segmentation and labelling

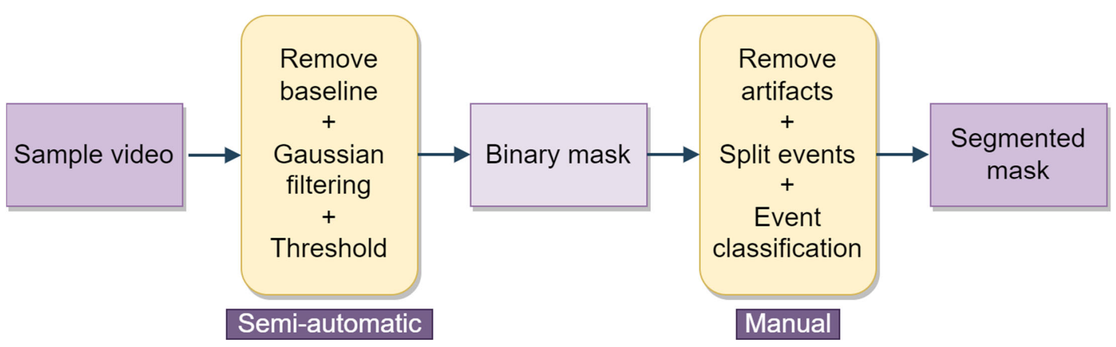

Figure 4: Data were manually annotated, with the help of a semi-automatic preprocessing of the samples.

3D U-Net input and architecture

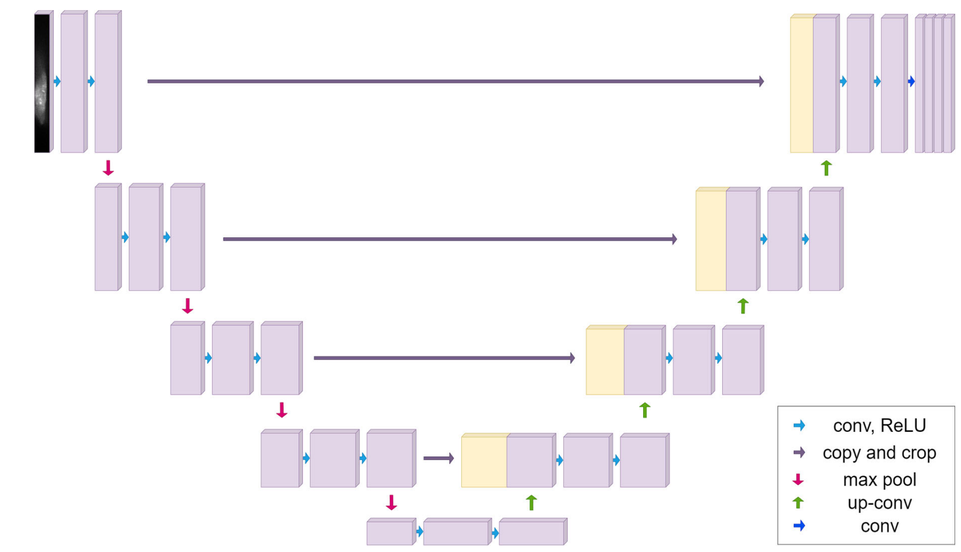

Figure 5: 3D U-Net architecture: the input is an extract of the input image series, and the output consists of 4 image series, representing the probability distribution for each class (events and background).

We split each sample into overlapping chunks of 256 frames, with a step of 32 frames. Data augmentation is done by flipping the samples vertically and/or horizontally. The neural network architecture is based on the standard U-Net architecture which has been adapted to handle 3-dimensional data (fig. 5).

Experiments and results

We trained the neural network for 100K epochs on the Lovász-Softmax loss [4], using the Adam optimizer.

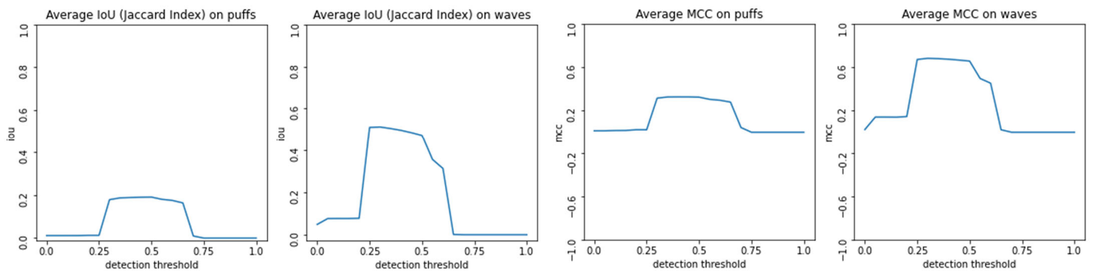

Figure 6a: average IoU (Jaccard Score) and Matthews correlation coefficient for **Ca^{2+} puff** and **Ca^{2+} wave** classes, with respect to detection threshold.

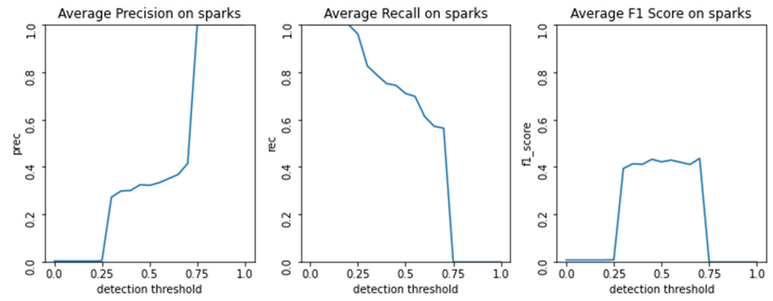

Figure 6b: average metrics for **Ca^{2+} spark** class, with respect to detection threshold.

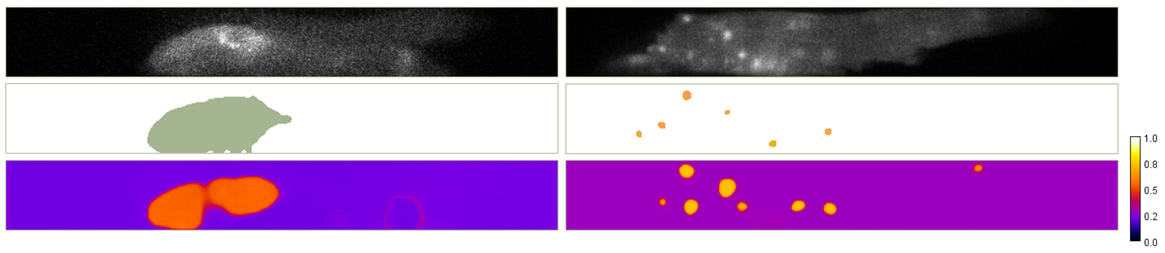

Figure 7: Example of the model's raw predictions. Left column: sample frame (top) with corresponding annotated Ca^{2+} wave, in green (center) and output of the network's softmax layer, for the Ca^{2+} waves class (bottom). Right column: sample frame (top) with corresponding annotated Ca^{2+} sparks, in orange, and Ca^{2+} puff, in yellow (center) and output of the network's softmax layer, for the Ca^{2+} sparks class (bottom).

Conclusion

- We present a novel approach to the detection and classification of local Ca^{2+} release events in cardiomyocytes.
- The trained network architecture provides a tool to solve this problem in a fully automated way, without manually processing xyt image series.
- Machine learning can help the detection and the categorization of local Ca^{2+} release.
- Further steps include the identification of the events in the prediction, and training with different types of neural network models.

References

[1] M. Wullschleger, J. Blanch, and M. Egger, "Functional local crosstalk of inositol 1,4,5-trisphosphate receptor- and ryanodine receptor-dependent Ca^{2+} release in atrial cardiomyocytes," Cardiovascular Research, vol. 113, pp. 542–552, 02 2017.

[2] H. Cheng, W. Lederer, and M. Cannell, "Calcium sparks: elementary events underlying excitation-contraction coupling in heart muscle," Science, vol. 262, no. 5134, pp. 740–744, 1993.

[3] I. Parker and Y. Yao, "Regenerative Release of Calcium from Functionally Discrete Subcellular Stores by Inositol Trisphosphate," Proceedings of the Royal Society of London Series B, vol. 246, pp. 269–274, Dec. 1991.

[4] M. Berman and M. B. Blaschko, "Optimization of the Jaccard index for image segmentation with the Lovász hinge," CoRR, 2017.